INVESTIGATION OF UNCOUPLED EFFECT OF MESH AND MODULUS ON MESENCHYMAL STEM CELL DIFFERENTIATION

A Senior Scholars Thesis

by

BAGRAT GRIGORYAN

Submitted to Honors and Undergraduate Research
Texas A&M University
in partial fulfillment of the requirements for the designation as

UNDERGRADUATE RESEARCH SCHOLAR

May 2012

Major: Biomedical Engineering

INVESTIGATION OF UNCOUPLED EFFECT OF MESH AND MODULUS ON MESENCHYMAL STEM CELL DIFFERENTIATION

A Senior Scholars Thesis

by

BAGRAT GRIGORYAN

Submitted to Honors and Undergraduate Research
Texas A&M University
in partial fulfillment of the requirements for the designation as

UNDERGRADUATE RESEARCH SCHOLAR

Approved by:

Research Advisor: Mariah Hahn
Associate Director, Honors and Undergraduate Research Duncan MacKenzie

May 2012

Major: Biomedical Engineering

ABSTRACT

Investigation of Uncoupled Effect of Mesh and Modulus on Mesenchymal Stem Cell Differentiation. (May 2012)

Bagrat Grigoryan
Department of Biomedical Engineering
Texas A&M University

Research Advisor: Dr. Mariah Hahn
Department of Chemical Engineering

Tissue engineering is an interdisciplinary field that aims to restore, maintain, or improve tissue function. Cells are incorporated into a scaffold that acts as a niche for the cells while they proliferate and differentiate into a specific cell type. Scaffold properties, such as mesh size and stiffness, have been demonstrated to impact cell behavior. However, since these properties are interdependent, identification of isolated scaffold effects on cell behavior has been proven to be difficult. For instance, an increase in molecular weight of a highly acrylated poly(ethylene glycol) diacrylated (PEGDA) results in an increase in the mesh and a decrease in the modulus of the resultant hydrogel. Due to this, attribution of expression of a specific cell type on a single parameter is complex. The aim of this study was to test the hypothesis that varying the acrylation of monomer, utilizing different photoinitiators, or incorporating a tetra-acrylated species could lead to formulations in which scaffold modulus and mesh size could be independently studied.

Formulations that demonstrate uncoupled mechanical and mesh properties will be selected for future cell studies to understand the influence of scaffold modulus and mesh size on cell behavior.

ACKNOWLEDGMENTS

I would like to thank my research advisor, Dr. Hahn, for her patience and guidance throughout my project.

I would also like to thank Dany, Carolina, Silvia, Viviana, and Chris for their help throughout the past year.

Also, I would like to thank my family for their encouragement and support.

NOMENCLATURE

COL1	Collagen I
COL2	Collagen II
Da	Dalton
DCM	Dichloromethane
DMEM	Dulbecco's modified eagle medium
ECM	Extracellular matrix
ELISA	Enzyme-linked immunosorbent assay
EtOH	Ethanol
hMSCs	Human mesenchymal stem cells
MW	Molecular weight
NMR	Nuclear magnetic resonance
PBS	Phosphate buffer saline
PEG	Poly(ethylene glycol)
PEGDA	Poly(ethylene glycol) diacrylated
PEGTA	Poly(ethylene glycol) tetra-acrylate
RT-PCR	Reverse transcription polymerase chain reaction
SEM	Scanning electron microscopy
SM	Smooth muscle
UV	Ultraviolet

TABLE OF CONTENTS

Page

LIST OF FIGURES

LIST OF TABLES

CHAPTER I

INTRODUCTION

Tissue engineering

Due to the low availability of organs for patients who require transplantation, the need for finding new sources for replacing or restoring physiological functions lost in damaged organs is high. Tissue engineering aims to resolve this issue by offering means to assemble tissue structures, under appropriate conditions, with the combination of cells and biomaterials. Ideally, a 3D scaffold containing previously isolated, cultured host cells is subjected to stimulation in a bioreactor that closely resembles the physiological environment, and then, implanted into the site of disease or damage in the patient's body (Figure 1)[1].

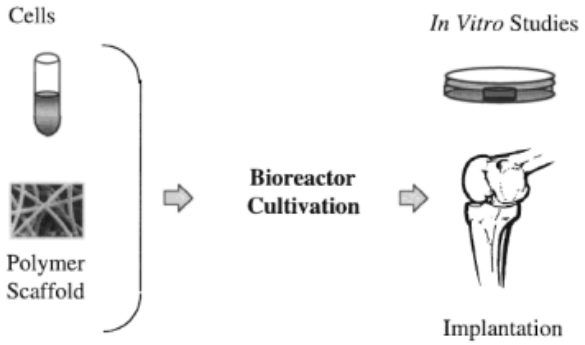

Figure 1. Depiction of the Tissue Engineering System. Cells isolated from cartilage tissue are cultured on a three-dimensional polymer scaffold using bioreactors. Then, the engineered tissue construct can be used for implantation[1].

This thesis follows the style and format of *Nature*.

These 3D scaffolds provide mechanical support, as well as chemical stimulation to the cells so that they may adhere, proliferate, and express specific phenotype markers. A wide variety of different materials have been utilized in tissue engineering. Metals and ceramics have been used advantageously in medical applications requiring superior mechanical properties, serving as a favorable choice in orthopedic applications. However, natural and synthetic polymeric materials are favorably used as scaffolds since their properties closely match the mechanical and biochemical properties of natural living tissue. Natural polymers, such as collagen, have been used extensively in tissue engineering and are available for clinical use in applications such as skin repair and nerve repair. Synthetic polymers circumvent limitations of natural polymers, such as biocompatibility and limited range of mechanical properties, due to their nature of high tunability[2].

Hydrogels

Hydrogels are three-dimensional, polymeric networks that closely resemble natural living tissue[3,4]. The polymeric networks are insoluble due to physical or chemical crosslinks, which maintain their network structure. Hydrogels are hydrophilic and can be tuned to absorb many times their dry weight in aqueous solution[5]. Depending on their chemistry and intended application, hydrogels can be either degradable or non-degradable. Chemically crosslinking may be achieved to prevent the dissolution of the polymer chains in an aqueous environment. A schematic of a crosslinked network is shown in Figure 2.

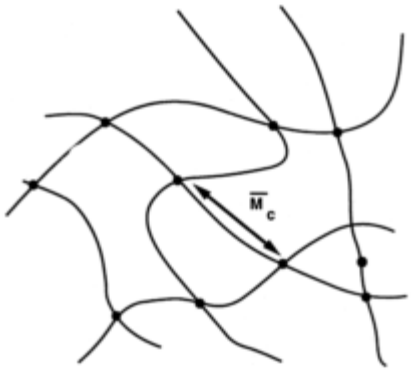

Figure 2. Representation of a crosslinked network. M_c is the molecular weight between crosslinks[6].

Chemically crosslinked polymers with vinyl groups (double bonds) may be obtained by polymerization while using a photoinitiator that becomes active when exposed to light of specific wavelength[7,8]. In photopolymerization, the polymer in the precursor solution is converted to a three-dimensional network. One way to achieve this is by photoinitiated radical polymerization, where radiation of the photoinitiator results in free radicals which are used to initiate and then propagate growing polymeric networks (Figure 3). In the initial step, photoinitiation, an initiator molecule absorbs light in either the ultraviolet or visible light range. The initiation of the chain polymerization reaction occurs when the excited photoinitiator molecule dissociates into primary radicals. In the second step of the chain polymerization reaction, the radicals are reacted with the polymer's vinyl groups and successively propagate, resulting in longer chains. The chain polymerization reaction terminates once polymer or free radicals are exhausted, forming a crosslinked network.

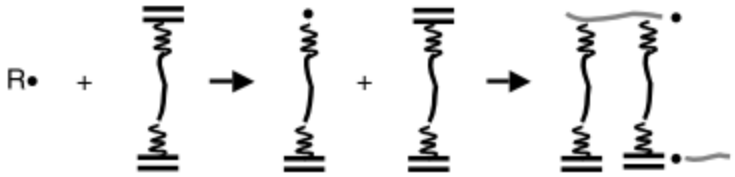

Figure 3. Network formation in polymers with vinyl groups by photopolymerization. A free radical reacts with the vinyl group of a polymer, resulting in propagation and chemical crosslinks[8].

Material properties

Selecting proper materials for the desired design requirements is crucial since the choice of contents in the precursor solution will influence the material properties[9–12]. The 3D morphology of the gel is determined by the polymer chemistry, crosslinking agent, and method of polymerization. A cryoSEM image of the architecture of a hydrogel is shown in Figure 4.

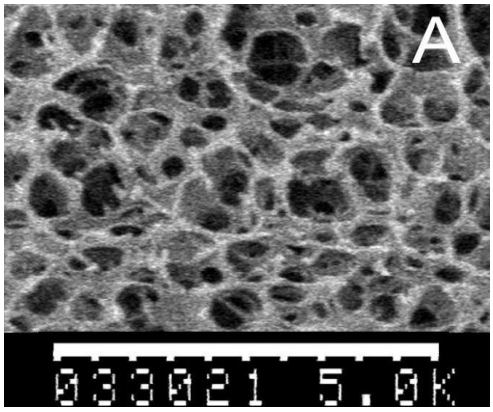

Figure 4. Interior morphology of poly(ethylene glycol) diacrylate hydrogel obtained from scanning electron microscopy[13].

Hydrogel properties, such as modulus and mesh size, are important to interpret since they affect cell behavior[14–17]. Mechanical properties such as the Young's Modulus, which measures the elasticity of a hydrogel, are important when designing a scaffold, since the network must be able to reinforce cells encapsulated or seeded onto a hydrogel. Mesh size of a hydrogel is another important factor since it can influence the mechanical strength and diffusivity of the network. Larger mesh sizes allow for nutrient transport into the network so that cells can proliferate or drugs can elute out into the surrounding environment. Generally, these properties are correlated; increase in modulus will result in a decrease in mesh size, while a decrease in modulus will result in an increased mesh size[18]. The identification of specific cell responses to isolated scaffold parameters is important since different tissues require different material properties for mechanical and biochemical support. For instance, bone repair and regeneration requires scaffold with high elastic modulus to support cell growth and development, while low elastic modulus is important for the maintenance of neural cells[19,20].

Due to their biocompatibility, tunability of material properties, and the ability to act as a blank slate, poly(ethylene glycol) (PEG) hydrogels have been widely used in tissue engineering applications[3,4,21]. PEG based hydrogels demonstrate a wide variety of tunable properties due to the ability to alter the components of the precursor solution. The alteration of either molecular weight or concentration of poly(ethylene glycol) diacrylate (PEGDA) can influence the scaffold modulus and mesh size[10,12]. By the addition of cell adhesion peptides, cell attachment is accomplished to the hydrogel

surface[15]. By lowering the acrylation of PEGDA, the desired effect of uncoupling scaffold modulus and mesh size has led to the production of different extracellular matrix (ECM) components[13].

Proposed research

The ability to decouple scaffold modulus and mesh size would allow for networks with either similar modulus or mesh size, leading to control identification of isolated effects on cell behavior. Therefore, the goal of this study is two-fold: (1) investigate an approach to isolate the effect of hydrogel modulus or mesh size in PEG hydrogels by incorporating low polymer acrylation, PEGTA, or altering photoinitiator to the precursor solution, and (2) propose methods to assess cell differentiation in formulations that demonstrate independent hydrogel modulus and mesh size. By tuning the contents of the precursor solution, the evaluation of separate influences of modulus and mesh size on cell response may be explored toward rational scaffold design.

Recently, it has been demonstrated that the acrylation of 4-star PEG into poly(ethylene glycol) tetra-acrylate (PEGTA) results in interdependence of scaffold modulus and mesh size, with minimal changes in mesh and distinct changes in modulus as PEGTA concentration increased[22]. However, cell studies have not been performed on those formulations that introduce the crosslinker. The choice of photoinitiator in the precursor solution can also be altered to result in modifications in the polymerized 3-D hydrogel, which may result in the desired uncoupling effect.

CHAPTER II

METHODOLOGY

Material characterization

Polymer synthesis

PEGDA was prepared as previously described by combining 0.1 mmol/mL dry PEG (3.4, 6.0, 8.0, 10, or 20 kDa, Fluka), 0.4 mmol/mL acryloyl chloride, and 0.2 mmol/mL triethylamine in anhydrous dichloromethane (DCM) and stirring under argon overnight (Figure 5)[23]. The resulting solution was washed with 2M K_2CO_3 and separated into aqueous and DCM phases to remove HCl. The DCM phase was subsequently dried with anhydrous $MgSO_4$, and PEGDA was precipitated in diethyl ether, filtered, and dried under vacuum.

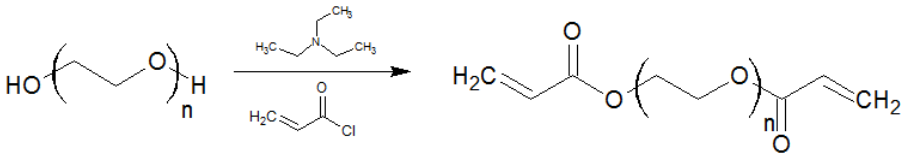

Figure 5. Schematic representing the synthesis of poly(ethylene glycol) diacrylate.

PEGTA was prepared by using the same method, but concentrations of the chemicals were adjusted due to the additional 2 end groups associated with the 4-arm PEG. Briefly, The tetra-acrylated 4-arm PEG was prepared by combining 0.1 mmol/mL dry PEG (2 kDa, Fluka), 0.4 mmol/mL acryloyl chloride, and 0.2 mmol/mL triethylamine in

anhydrous DCM and stirring under argon overnight (Figure 6). The resulting solution was washed with 2M K_2CO_3 and separated into aqueous and DCM phases to remove HCl. The DCM phase was subsequently dried with anhydrous $MgSO_4$, and 4-arm PEGTA was precipitated in diethyl ether, filtered, and dried under vacuum.

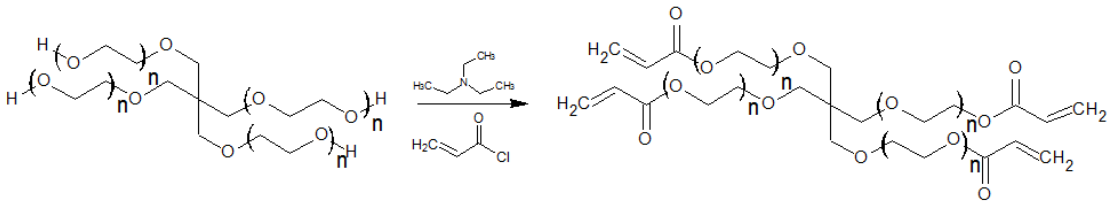

Figure 6. Schematic representing the synthesis of 4-arm poly(ethylene glycol) tetra-acrylate.

Linear PEGDA and 4-arm PEGTA functionalization was confirmed using proton nuclear magnetic resonance (^{1}H NMR). The extent of acrylation was characterized to be higher than 90% for all synthesized polymers.

Hydrogel formation

High and low acrylated PEGDA molecular weights of 6.0, 8.0, 10, and 20 kDa at concentrations of 5, 10, 15, 20, 25, and 30% were investigated in this study. In addition, some formulations consisted of 2 kDa 4-arm PEGTA that were added at a ratio of either 25:75 or 75:25 PEGDA to PEGTA. Precursor solutions were prepared by dissolving PEGDA in phosphate buffer saline (PBS), and adding a photoinitiator (Irgacure 2959 in 70% EtOH at concentration of 260 mg/ml, or Irgacure 651 in NVP at concentration of

300 mg/ml) at 10 ul/mL precursor solution. Chemical structures of the two photoinitiators are shown in Figure 7. Irgacure 2959 in EtOH at concentration of 260 mg/ml was used for formulations that contained a mixture of the 4-arm PEGTA and PEGDA. Formulations with lower acrylation levels were obtained by adding mono-acrylated PEG and non-acrylated PEG to PEGDA, creating a polymer blend, at a specific ratio, depending on the probability of functionalization. Each precursor solution was poured into molds consisting of glass plates separated by polycarbonate spacers, and then polymerized by exposing to longwave UV light (Ultraviolet Products High Performance UV Transilluminator, ~6 mW/cm^2, 365 nm). Formulations that contained Irgacure 2959 were polymerized for 3 minute on each side, while formulations that contained Irgacure 651 were polymerized for 1 minute on each side. The hydrogels were then allowed to swell in PBS for 24 hours before further analysis.

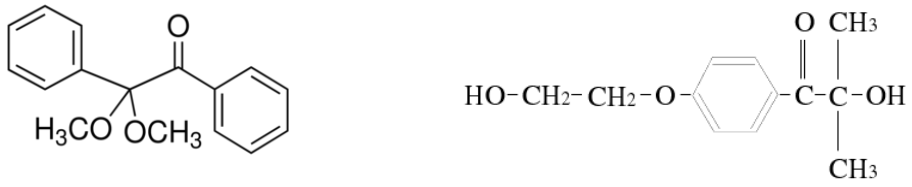

Figure 7. Left: Chemical structure of Irgacure 651. Right: Chemical structure of Irgacure 2959.

Hydrogel mechanical properties

Samples from each hydrogel were obtained by punching the gels into 8 mm diameter punches (n=4). An Instron Mechanical Tester 3342 was used to perform tensile testing of the sample at a rate of 0.15 mm/sec following. The Young's Modulus was calculated

from the resulting data by obtaining the slope of the linear portion of the stress versus strain curve.

Hydrogel mesh size

Since PEG hydrogel mesh size can only be visualized using cryoSEM, which is expensive and time consuming. For this study, hydrogel mesh size was characterized by a series of dextran diffusion experiments which is relatively inexpensive[24,25]. Punched samples (n=4) were immersed in fluorescently tagged dextran of molecular weights 4, 10, and 20 kDa to allow dextran to diffuse into the gel. After 24 hours, each sample was gently blotted and then transferred to PBS for 24 hours. During those 24 hours, dextran that had penetrated into the hydrogels was permitted to diffuse out into the surrounding solution. The fluorescence of the PBS solution surrounding each gel was tested by using a microplate reader at ex/em 488/532. Standard curves were used to obtain the concentration of penetrated dextran from the fluorescence signal, from which the relative mesh size was extrapolated. A schematic of the technique is shown in Figure 8.

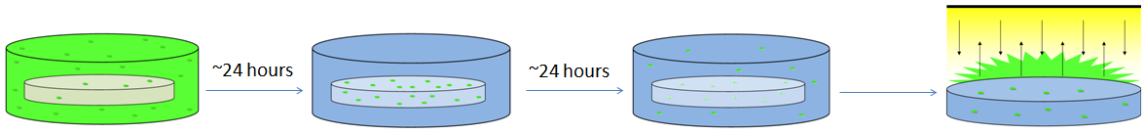

Figure 8. Schematic illustrating dextran diffusion technique. Gels are submerged in a fluorescently labeled dextran and allowed to reach equilibrium overnight. Then, gels are transferred to PBS and allowed to reach equilibrium overnight. The fluorescence of the PBS elution is then measured and converted to a corresponding concentration by using standard curves.

For each hydrogel formulation, the measured concentration readings for each dextran MW were divided by gel weight. Then, the resulting data was plotted against the MW for the dextran used. The total area under the resulting curve serves as a quantitative indicator of hydrogel permissivity. The mesh size of each gel formulation was obtained relative to that of the 10% 10kDa hydrogel formulation.

Cell response characterization

Two-dimensional monolayer studies

Human mesenchymal stem cells (hMSCs) (Lonza, Walkersville MD) from a 24 year old female were used in cell studies. This 2D study was performed in order to develop and validate the methods to investigate the gene expression profiling on cultured hMSCs.

Cell culture conditions

hMSCs were plated in six-well tissue culture plates and allowed to reach confluence. Cells were grown in either MesenPRO RS media (Invitrogen, Carlsbad CA) as the undifferentiated control set as well as adipogenic, osteogenic, chondrogenic, or DMEM media supplemented with TGF-β1 (Lonza, Walkersville MD).

Purification of mRNA

Isolation of mRNA was performed using Dynabeads® DNA DIRECT^{TM} Kit (Invitrogen, Carlsbad CA). Instructions supplied with the kit were followed. Purified mRNA was stored at -80 °C until further use.

Quantitative reverse transcription polymerase chain reaction (qRT-PCR)

Reverse transcription was performed using SuperScript III Platinum One-Step qRT-PCR kit for qRT-PCR (Invitrogen, Carlsbad CA). A control containing no reverse transcriptase was also performed to verify absence of contaminating genomic DNA. Reverse transcription yielded cDNA, which was then utilized in the polymerase chain reaction (PCR).

qRT-PCR was used to assess and confirm pluripotency of hMSCs used in this study as well as primer performance for selected differentiation markets. Adipogenic markers included peroxisomes proliferator-activated receptor gamma (PPARG), adipsin, and adipocyte fatty acid binding protein (AFABP). Chondrogenic markers included SOX9 and collagen type II (COL2). Smooth muscle markers included SM22-alpha, calponin, and SM-alpha actin. Osteogenic markers included osteocalcin, osteopontin, RUNX2, and collagen type I (COL1).

Polymerase chain reactions were conducted using reagents and primers obtained from Invitrogen according to instructions provided with StepOne Real Time PCR System for qRT-PCR.

Statistical analysis

All data are reported as mean ± standard deviation. Comparison of sample means was performed using ANOVA and Tukey‘s post-hoc test (SPSS software), $p < 0.05$.

CHAPTER III

RESULTS

Hydrogel properties

Hydrogel mechanical properties and mesh size were characterized for PEGDA hydrogels by varying molecular weight, polymer concentration, photoinitiator system, acrylation level, and addition of crosslinker.

Effect of varying polymer concentration and molecular weight

To investigate whether varying polymer concentration and molecular weight in formulations that consisted of Irgacure 651 would result in the desired uncoupling effect, tensile testing was performed and the modulus was calculated from the linear portion of the resulting stress-strain curve (Figure 9). Corresponding mesh size estimation in Irgacure 651 gels was assessed by dextran diffusion (Figure 10). Increasing molecular weight of PEGDA used resulted in a decrease in modulus, coupled with a increase in mesh size. Increasing polymer concentration resulted in an increase in modulus, coupled with a decrease in mesh size.

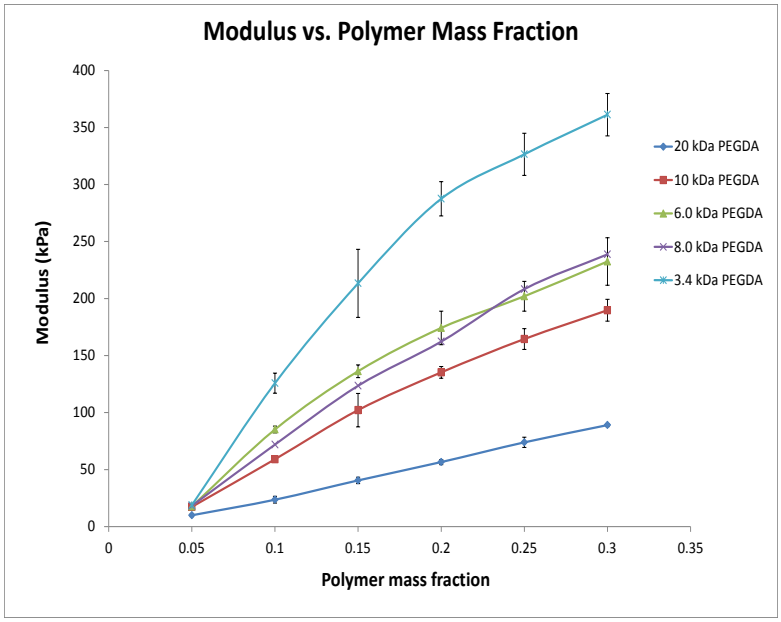

Figure 9. Modulus of Irgacure 651 hydrogels of varying polymer concentration and molecular weight.

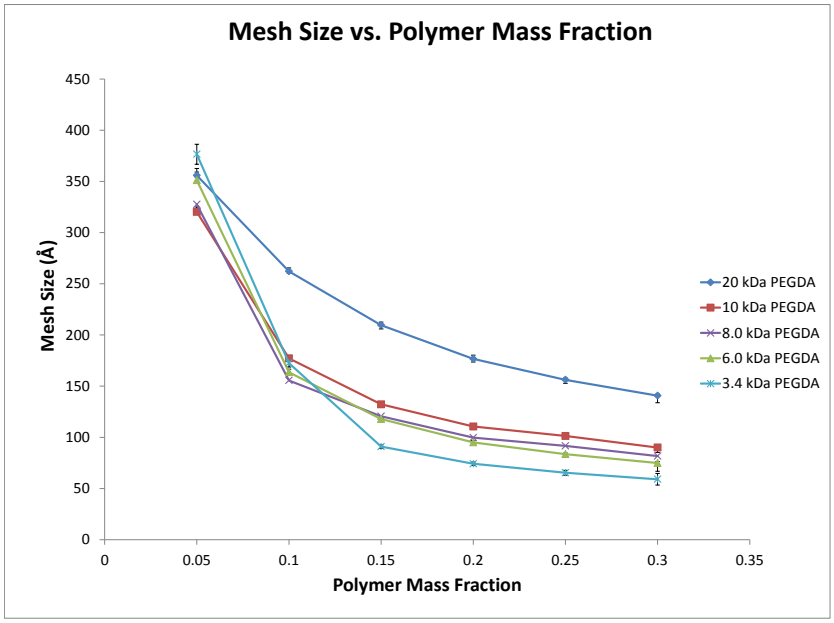

Figure 10. Mesh size estimation of Irgacure 651 hydrogels of varying polymer concentration and molecular weight.

Effect of varying photoinitiator

Three formulations were chosen randomly for further analysis (10 kDa PEGDA 10%, 10 kDa PEGDA 20%, and 20 kDa PEGDA 30%). To investigate the modulation of modulus by varying photoinitiator systems, tensile testing was performed and the modulus was calculated from the linear portion of the resulting stress-strain curve (Figure 11). To investigate the modulation of mesh size by varying photoinitiator systems, dextran diffusion testing was performed on hydrogels with varying photoinitiator (Figure 12). Irgacure 651 system resulted in a higher modulus, coupled with a lower mesh size.

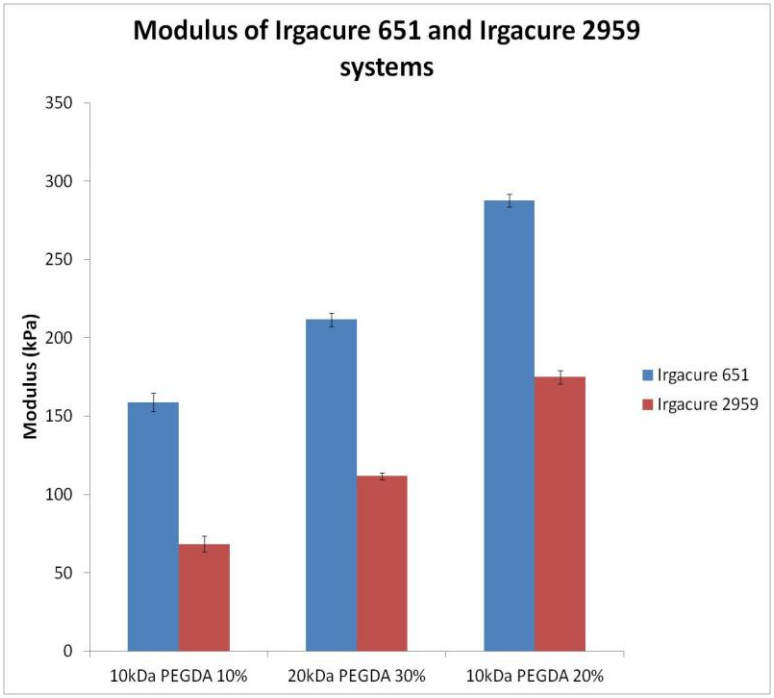

Figure 11. Mechanical properties of hydrogels in Irgacure 651 and Irgacure 2959.

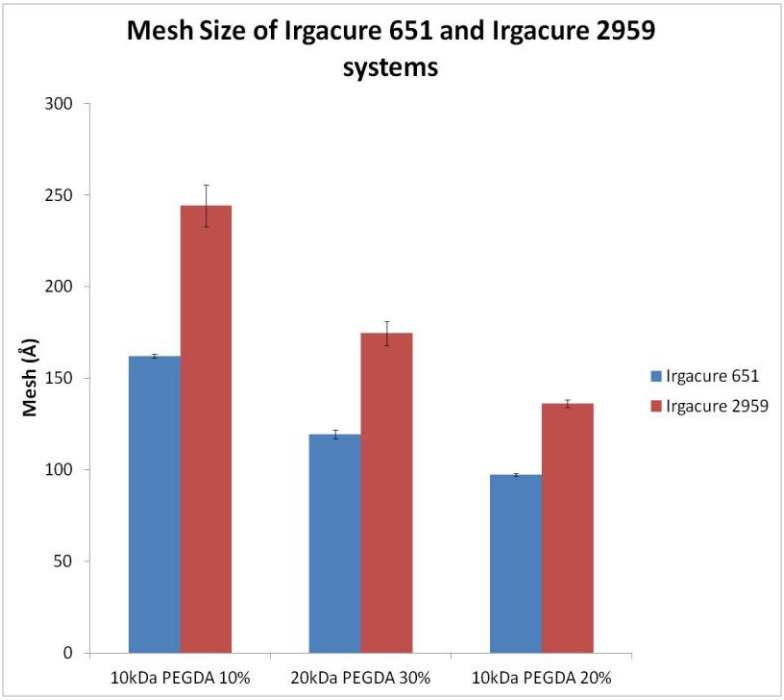

Figure 12. Mesh size of hydrogels in Irgacure 651 and Irgacure 2959 systems.

Effect of varying acrylation level

To investigate whether varying photoinitiator content would result in uncoupling effect, the modulus was obtained from formulations that contained low acrylated and high acrylated species in Irgacure 651 (Figure 13) and Irgacure 2959 (Figure 15). Dextran diffusion was used to estimate the mesh of formulations that contained low acrylated and high acrylated species in Irgacure 651 (Figure 14) and Irgacure 2959 (Figure 16). Lower acrylation resulted in a lower modulus, coupled with a higher mesh size for both photoinitiator systems.

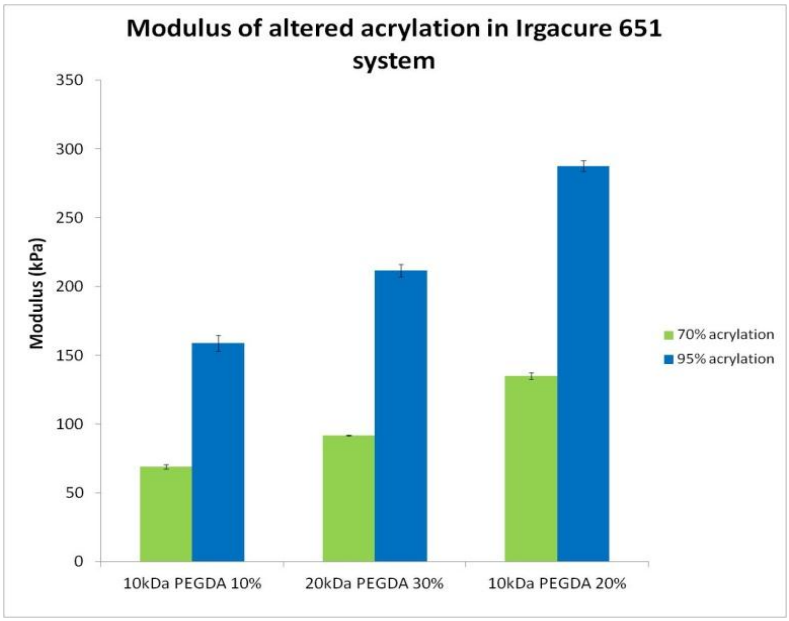

Figure 13. Mechanical properties of low and high acrylated species in Irgacure 651.

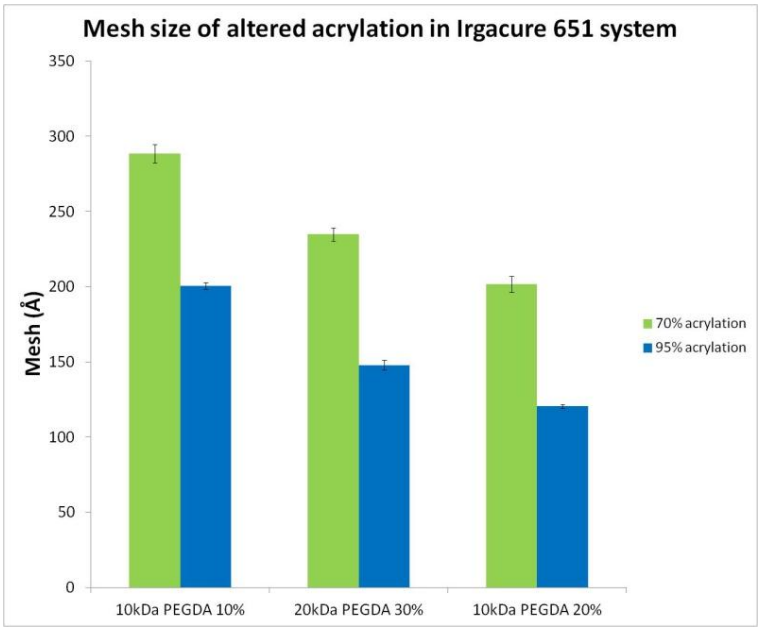

Figure 14. Mesh size estimation of low and high acrylated species in Irgacure 651.

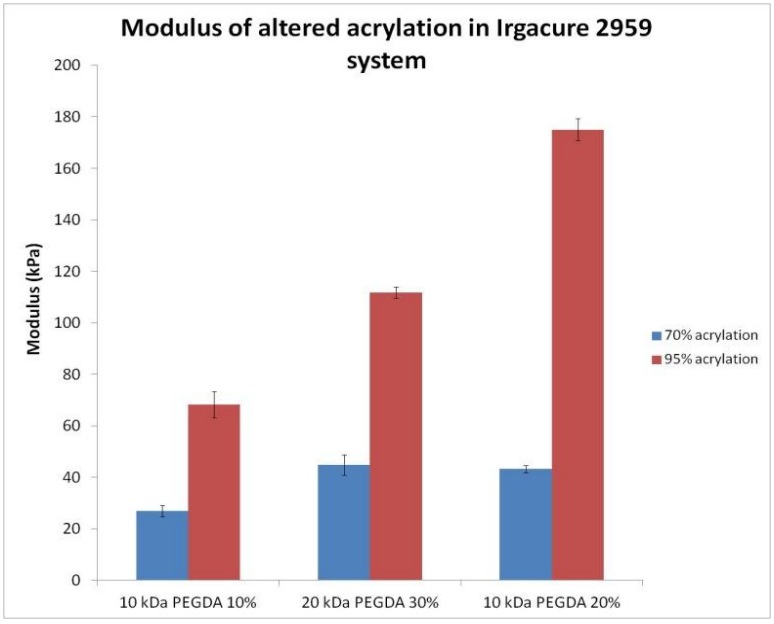

Figure 15. Mechanical properties of low and high acrylated species in Irgacure 2959.

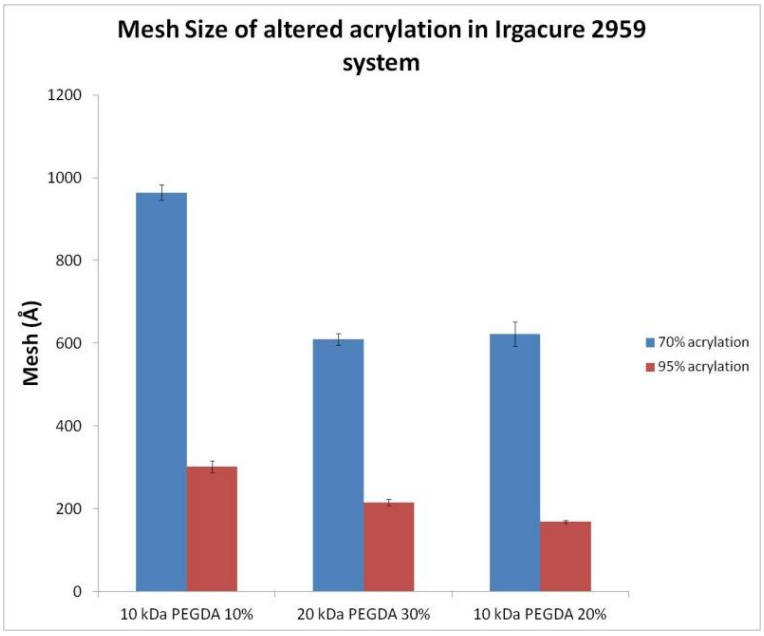

Figure 16. Mesh size of low and high acrylated species in Irgacure 2959.

Effect of addition of crosslinker

The effect of incorporation of crosslinker 4-arm PEGTA on modulus was determined by calculating the linear portion of the stress strain curve (Figure 17). The effect of incorporation of crosslinker 4-arm PEGTA on mesh size was determined by performing dextran diffusion (Figure 18). Introduction of crosslinker in 6 kDa 20% formulation did not result in modulation of modulus, however, mesh size varied. For the higher molecular weight PEGDA used, addition of crosslinker influenced the mechanical properties, as well as mesh size.

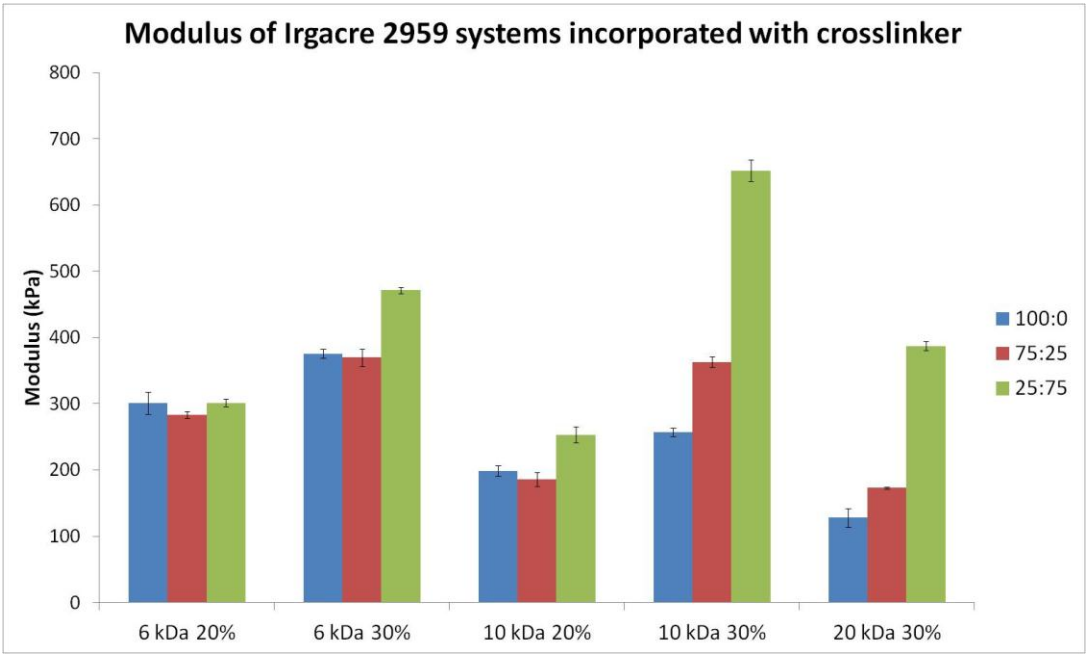

Figure 17. Mechanical properties of hydrogels with crosslinker.

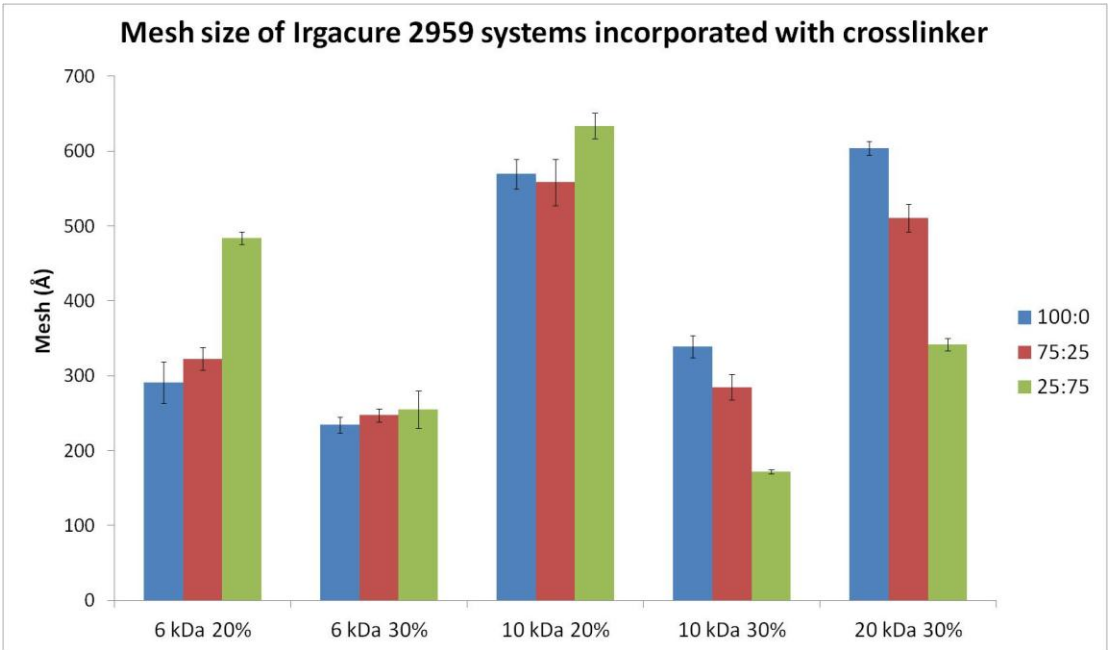

Figure 18. Relative mesh size estimation of hydrogels with crosslinker.

Comparison of modulus and mesh

The modulus of formulations in which polymer concentration, polymer molecular weight, initiator, and acrylation were altered was plotted versus its respective mesh size (Figure 19).

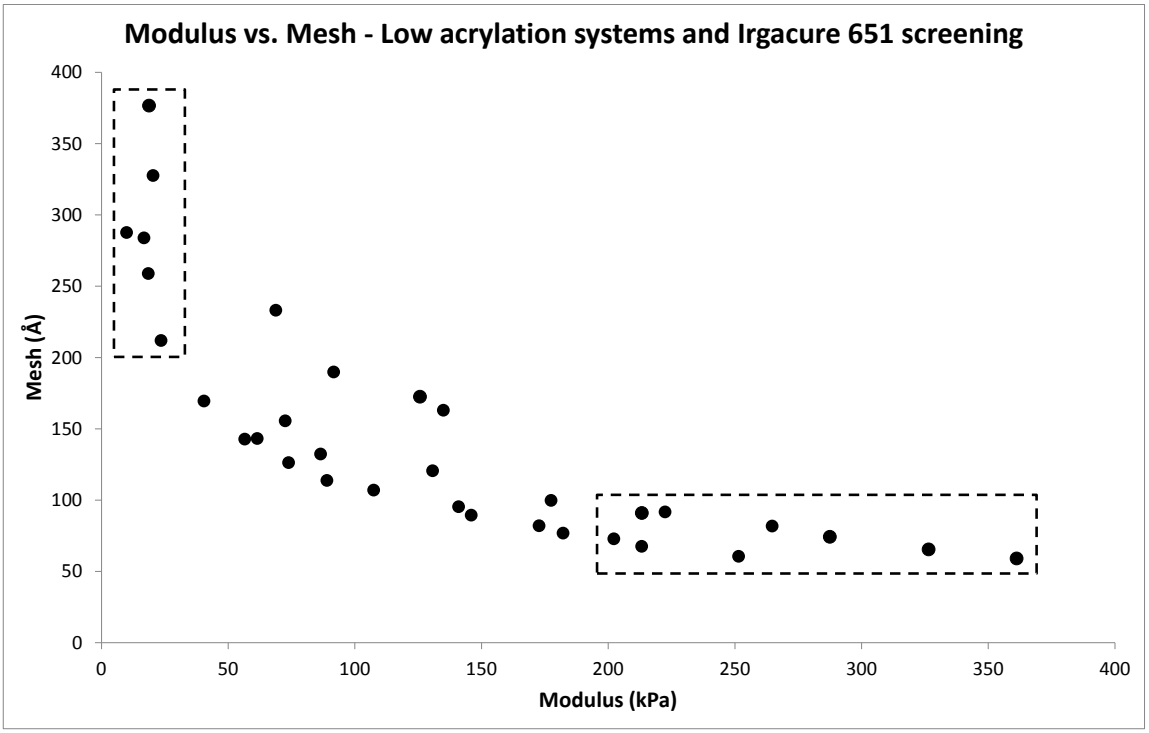

Figure 19. Modulus versus mesh of formulations in which precursor content was varied, demonstrating the ability to isolate formulations in which modulus and mesh size have been uncoupled. Dashed boxes represent a subset of formulations in which formulations demonstrated similar modulus, different mesh size and similar mesh size, different modulus.

Examples of some formulations that demonstrated the desired changes in modulus and mesh size are summarized in Table 1.

Table 1. Examples of formulations in which polymer concentration, polymer molecular weight, acrylation level, and photoinitiator was altered and uncoupling of properties was observed.

	Formulation	Properties	
		Modulus (kPa)	Mesh (Å)
Similar modulus, different mesh size	6 kDa PEGDA 10%, Irgacure 651	86.5 ± 3.2	132.2 ± 2.0
	20 kDa PEGDA 30%, Irgacure 651	89.0 ± 1.3	113.7 ± 0.7
Similar mesh size, different modulus	20 kDa PEGDA 15%, Irgacure 651	40.5 ± 2.8	169.4 ± 1.8
	10 kDa PEGDA 20%, 70% acrylation, Irgacure 651	135.0 ± 2.5	163.0 ± 4.0

In addition, the modulus of formulations that incorporated the crosslinker was plotted versus its respective mesh size (Figure 20).

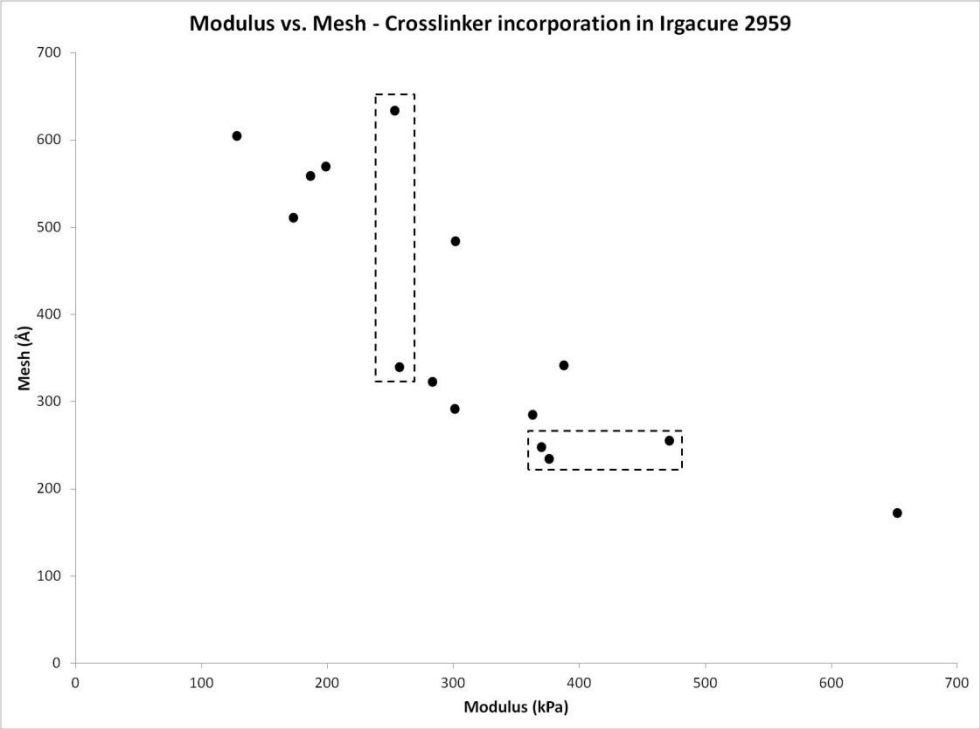

Figure 20. Modulus versus mesh of formulations in which a crosslinker was incorporated, demonstrating the ability to isolate formulations in which modulus and mesh size have been uncoupled. Dashed boxes represent a subset of formulations in which formulations demonstrated similar modulus, different mesh size and similar mesh size, different modulus.

Examples of formulations that demonstrated the desired changes in modulus and mesh size after incorporation of crosslinker are summarized in Table 2.

Table 2. Examples of formulations in which crosslinker was incorporated into the network and uncoupling of properties was observed.

	Formulation	Properties	
		Modulus (kPa)	Mesh (Å)
Similar modulus, different mesh size	10 kDa PEGDA 30%, 100:0 PEGDA:PEGTA	257 ± 6.5	339.3 ± 14.8
	10 kDa PEGDA 20%, 25:75 PEGDA:PEGTA	253.3 ± 12.1	633.8 ± 17.3
Similar mesh size, different modulus	10 kDa PEGDA 30%, 100:0 PEGDA:PEGTA	257 ± 6.5	339.3 ± 14.8
	20 kDa PEGDA 30%, 25:75 PEGDA:PEGTA	387.3 ± 6.7	341.7 ± 8.3

Cell response characterization

RT-PCR conditions and primer validation for gene expression profiles analysis of hMSCs was performed. Adipogenic (PPARG, adipsin, AFABP), chondrogenic (SOX9, COL2), osteogenic (osteocalcin, osteopontin, RUNX2, COL1) and SM (SM22-alpha, calponin, SM-alpha actin) primers for differentiation markers were tested for primer specificity, and performance was confirmed using RNA control samples. Representative amplification and melting curve of one of the tested primers, RUNX2, are shown in Figure 21 and Figure 22, respectively.

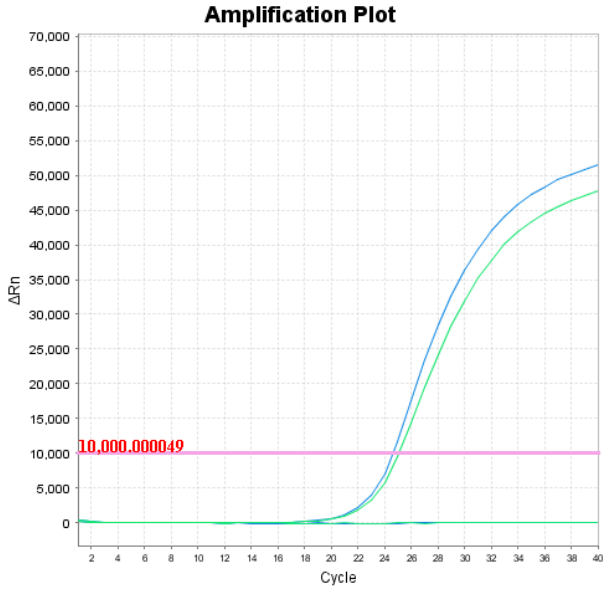

Figure 21. Amplification plot of RUNX2.

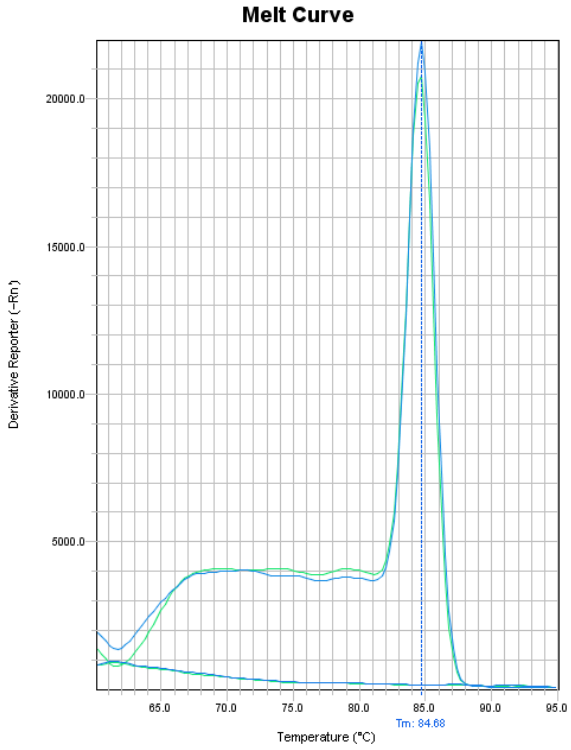

Figure 22. Melting curve of RUNX2.

CHAPTER IV

DISCUSSION

Hydrogel properties

Tensile testing was used to obtain the modulus of formulations with varying precursor solution contents. Since visualizing PEG based hydrogel mesh size by using techniques such as cryoSEM is expensive and difficult to, a series of dextran diffusion experiments was used to estimate mesh size in PEG hydrogels.

By varying polymer concentration and polymer molecular weight in the Irgacure 651 formulations, modulus and mesh size properties were modulated. As expected, increase in polymer concentration resulted in an increase in modulus, coupled with a decrease in relative mesh size. The increase in modulus with decrease in mesh size can be attributed to the increase in crosslink density as concentration of reactive polymer in the precursor solution is increased. Also, an increase in polymer molecular weight resulted in a decrease in modulus, coupled with an increase in relative mesh size. This decrease in modulus with an increase in mesh size can be attributed to the lower crosslink density and higher flexibility as chain length is increased.

By varying photoinitiator content, modulus and mesh size properties were varied. Formulations that consisted of Irgacure 651 resulted in an increase in modulus when

compared to Irgacure 2959. The relative mesh size of hydrogels with Irgacure 651 was significantly lower when compared to hydrogels with Irgacure 2959. This can be attributed to the higher efficiency of Irgacure 651 system compared to Irgacure 2959 system. Also, the Irgacure 651 system involved NVP, which could be incorporated into the network.

Acrylation level was modified and the modulus and mesh size were investigated in formulations with Irgacure 651 and Irgacure 2959. In both cases, the lower acrylated formulations resulted in hydrogels with a decrease in modulus, coupled with an increase in mesh size. This decrease in modulus can be attributed to the lower crosslink density due to a decrease in reactive functional groups. When comparing the two different photoinitiators, the hydrogels with Irgacure 651 resulted in a higher modulus, coupled with a decrease in mesh size.

Incorporation of additional crosslinker was used to investigate the effects of modulus and mesh size of corresponding hydrogels. In 30% 10 kDa and 20 kDa formulations, increasing the amount of crosslinker incorporated into the network resulted in significant modulation of hydrogel properties. This can be attributed to the average molecular weight of the polymer blend, which is higher for the higher PEGDA molecular weight formulations. Interestingly, the 6 kDa PEGDA 30% 25:75 PEGDA:PEGTA formulation resulted in a lower modulus when compared to the 10 kDa PEGDA 30% 25:75

PEGDA:PEGTA. Increasing the amount of crosslinker into the network also resulted in a modulation of the relative mesh size. Another unexpected result was the trend of the 30% polymer concentration hydrogels with 25:75 PEGDA:PEGTA. Instead of a steady increase in mesh size from 6 to 20 kDa PEGDA, the 10 kDa hydrogel resulted in a lower mesh size when compared to the 6 kDa hydrogel.

Cell response characterization

Development of techniques to assess gene expression profiles was performed. Primers for differentiation markers were confirmed in 2-D studies. High quality and purity level of mRNA were achieved since low Ct value from the amplification curve was observed and no amplification of genomic contamination control was observed. High primer specificity was confirmed from single peak in the dissociation curve, indicating a single amplification. Single melting temperature and temperature values over 80°C suggest absence of primer dimmer which are normally associated with peak at low temperatures values around 70°C.

CHAPTER V

FUTURE WORK

Cell studies

Cell encapsulation

3-D studies involving hMSC encapsulation will be performed on formulations that demonstrated the desired modulus and mesh uncoupling effect. Hydrogel fabrication for 3-D studies will involve the addition of 1 mM ACRL-PEG-RGDS in the precursor solution. Harvested and resuspended hMSCs 1 x 10^6 cells/ml will be transferred to filter-sterilized precursor solutions prior to exposure to UV light. Polymerized hydrogels will be immersed in either the control MesenPRO RS media or specific differentiation media (adipogenic, chondrogenic, smooth muscle, or osteogenic), maintained at 37°C/5% CO_2. The medium will be changed every 2 days, for 21 days.

Construct analyses

After 21-day total culture time, constructs will be harvested for mechanical and biochemical analyses. To preserve sample RNA, construct segments will be immersed in RNA-later and stored at 4°C overnight, per manufacturer's instructions, before transfer to -80°C.

RNA isolation

Hydrogels preserved in RNA-later will be removed from 80°C and transferred to 2 mL screw-cap microfuge tubes containing 1.5mL of Trizol reagent (Invitrogen, Carlsbad,

CA) and 1mL of 3.2mm stainless steel beads. Each sample segment will be homogenized at 4800 rpm in a Bead-Beater homogenizer (Biospec, Bartlesville, OK) in 10 s cycles with 1 min intermediate cooling on ice. The resulting solutions will be centrifuged, and the supernatants will be mixed with chloroform (Sigma), vigorously shaken for 15 s, and centrifuged. The upper aqueous phases of all segments of a given sample will be combined and collected, and the lower phenol–chloroform phases will be stored at -20°C for subsequent protein isolation.

RNA will be precipitated from the aqueous phase using isopropanol, with RNase-free glycogen added as a carrier. The resulting pellet will be sequentially washed with 75% and 95% ethanol and then exposed to DNase (Qiagen, Valencia, CA) at 37°C. After 30 min digestion, the mixture will be transferred to 70°C for 5 min to inactivate the DNase enzyme, and then immediately chilled on ice. RNA will be precipitated by adding 10 mL of 3 M sodium acetate (pH 5.5) followed by 275 mL of 100% ethanol per 100 mL of digestion mixture. The pellet will then be sequentially washed with 75% and 95% ethanol and then resuspended in 51 μL of RNase-free water[5].

Quantitative RT-PCR

qRT-PCR was performed on each sample using a StepOne Real Time PCR System detection system (Biorad, Hercules, CA) and the SuperScript III Platinum One-Step qRT-PCR kit (Invitrogen). mRNA levels for each gene of interest were assessed in duplicate for each construct. Six microliters of template and 5 μL of 1 μM primer were

added per 25 μL reaction mixture. Amplification during the PCR phase was monitored by measuring the change in SYBR Green fluorescence. A threshold fluorescence value at which each sample was in the exponential phase of amplification was identified using MyiQ software (Biorad). The amplification cycle at which a given sample crossed this threshold was recorded as the Ct for that sample. For each construct, $2^{-\Delta Ct,gene} = 2^{-(Ct,gene-Ct,GAPDH)}$ was calculated for genes osteocalcin, osteopontin, RUNX2, collagen type I, PPARG, adipsin, AFABP, SM22-alpha, calponin, SM-alpha actin, SOX9, and collagen type II as a quantitative indicator of their expression levels relative to housekeeping gene GAPDH. The average $2^{-\Delta Ct,gene}$ value for a given gene and treatment group was then normalized by the corresponding average $2^{-\Delta Ct,gene}$ for the constructs. Melting curve analysis will be performed for each reaction to verify a single product of the correct size[5].

Protein isolation

Protein isolation will be performed for analysis of protein and phenotype expression. Sample proteins will be isolated using a modification of a procedure validated by Hummon *et al*[26]. In brief, the phenol–chloroform phase resulting from each Trizol-based RNA extraction will be mixed with ethanol to precipitate residual DNA. The resulting phenol–ethanol phases will be transferred to 3.4 kDa SnakeSkin dialysis membranes (Pierce, Rockford, IL). The solutions will be dialyzed for ~60 h at 4°C against an aqueous solution of 0.1% sodium dodecyl sulfate (SDS), with buffer exchange every ~18–20 h. By the end of third 18–20 h dialysis period, the samples will be partitioned

into three phases: (1) a supernatant, (2) a globular mass, and (3) a colorless, viscous liquid. Each globular mass, containing the bulk of sample proteins, will be collected and resuspended in PBS containing 0.5% SDS and 1% Triton X-100[26].

Biochemical analysis

Enzyme-linked immunosorbent assay (ELISA) will be utilized to assess the differentiation of hMSCs into specialized cell types. Primary antibodies and their corresponding peptide antigens will be purchased from Santa Cruz Biotechnology (SCBT). High binding EIA 96 well plates (Costar) will be coated overnight at 4°C with 2 ng per well of peptide for specific markers expressing bone (osteopontin, osteocalcin, RUNX2, collagen type I), cartilage (SOX9, collagen II), muscle (SM22-alpha, calponin, SM-alpha actin), and fat tissue (PPARG, adipsin, AFABP) will be used to detect different cell types. The coated wells will then blocked with bovine serum albumin (BSA). Peptide standards and resuspended protein samples will be diluted in PBS containing 3% BSA and 0.05% Tween 20 and incubated with primary antibody for 1 h at room temperature prior to transfer to the coated wells. The plate will then be incubated for 1 h at room temperature with continuous gentle mixing, after which HRP-conjugated secondary antibody (Jackson Immunochemicals) will be applied to each well. Levels of antigen in each sample will be evaluated indirectly via measuring the amount of secondary antibody bound to each well. This will be quantified by the addition of 2,2'-azino-bis(3-ethylbenzthiazoline-6-sulphonic acid) and subsequent absorbance measurements at 410 nm. ELISA results will be normalized to sample total protein as

determined using the CBQCA assay (Invitrogen) per manufacturer protocol. Samples will be measured in duplicate.

CHAPTER VI

CONCLUSION

The identification of specific cell responses to isolated scaffold parameters is important to characterize since different tissues require different material properties for mechanical and biochemical support. In this study, an extensive library of formulations were characterized by varying polymer concentration, molecular weight, acrylation level, photoinitiator, and crosslinker. Indeed, hydrogel formulations that demonstrated similar modulus but varied mesh size, and similar mesh size but varied modulus were identified. In the future, hMSC will be encapsulated in these uncoupled formulations to investigate the influence of isolated modulus and mesh size on cell behavior.

REFERENCES

1. Lanza, R., Langer, R.S. & Vacanti, J.P. *Principles of Tissue Engineering*. 144 (Academic Press: 2000).

2. Lavik, E. & Langer, R. Tissue engineering: current state and perspectives. *Applied Microbiology And Biotechnology* **65**, 1-8 (2004).

3. Graham, N.B. & McNeill, M.E. Hydrogels for controlled drug delivery. *Biomaterials* **5**, 27-36 (1984).

4. Liao, H. *et al.* Influence of hydrogel mechanical properties and mesh size on vocal fold fibroblast extracellular matrix production and phenotype. *Acta Biomaterialia* **4**, 1161-1171 (2008).

5. Hoffman, a S. Hydrogels for biomedical applications. *Annals of the New York Academy of Sciences* **944**, 62-73 (2001).

6. Ratner, B.D., Hoffman, A.S., Schoe, F.J. & Lemons, J.E. *Biomaterials Science - An Introduction to Materials in Medicine*. *Chemical Engineering* (2004).

7. Fisher, J.P., Dean, D., Engel, P.S. & Mikos, A.G. PHOTOINITIATED POLYMERIZATION OF BIOMATERIALS. *Annual Review of Materials Research* **31**, 171-181 (2001).

8. Ma, P.X. & Elisseeff, J.H. *Scaffolding in Tissue Engineering*. (CRC Press: 2006).

9. Peppas, N.A., Bures, P., Leobandung, W. & Ichikawa, H. Hydrogels in pharmaceutical formulations. *European journal of pharmaceutics and biopharmaceutics* **50**, 27-46 (2000).

10. Temenoff, J.S., Athanasiou, K.A., LeBaron, R.G. & Mikos, A.G. Effect of poly(ethylene glycol) molecular weight on tensile and swelling properties of oligo(poly(ethylene glycol) fumarate) hydrogels for cartilage tissue engineering. *Journal of biomedical materials research* **59**, 429-37 (2002).

11. Iza, M., Stoianovici, G., Viora, L., Grossiord, J.L. & Couarraze, G. Hydrogels of poly(ethylene glycol): mechanical characterization and release of a model drug. *Journal of Controlled Release* **52**, 41-51 (1998).

12. Ju, H., McCloskey, B.D., Sagle, A.C., Kusuma, V.A. & Freeman, B.D. Preparation and characterization of crosslinked poly(ethylene glycol) diacrylate hydrogels as fouling-resistant membrane coating materials. *Journal of Membrane Science* **330**, 180-188 (2009).

13. Munoz-Pinto, D.J., Bulick, A.S. & Hahn, M.S. Uncoupled investigation of scaffold modulus and mesh size on smooth muscle cell behavior. *Journal of Biomedical Materials Research Part A* **90A**, 303-316 (2009).

14. Bryant, S.J., Chowdhury, T.T., Lee, D.A., Bader, D.L. & Anseth, K.S. Crosslinking Density Influences Chondrocyte Metabolism in Dynamically Loaded Photocrosslinked Poly(ethylene glycol) Hydrogels. *Annals of Biomedical Engineering* **32**, 407-417 (2004).

15. Peyton, S.R., Raub, C.B., Keschrumrus, V.P. & Putnam, A.J. The use of poly(ethylene glycol) hydrogels to investigate the impact of ECM chemistry and mechanics on smooth muscle cells. *Biomaterials* **27**, 4881-4893 (2006).

16. Stegemann, J.P., Hong, H. & Nerem, R.M. Mechanical, biochemical, and extracellular matrix effects on vascular smooth muscle cell phenotype. *Journal of applied physiology (Bethesda, Md. : 1985)* **98**, 2321-7 (2005).

17. Kloxin, A.M., Kloxin, C.J., Bowman, C.N. & Anseth, K.S. Mechanical Properties of Cellularly Responsive Hydrogels and Their Experimental Determination. *Advanced Materials* **22**, 3484-3494 (2010).

18. Bryant, S.J. & Anseth, K.S. Hydrogel properties influence ECM production by chondrocytes photoencapsulated in poly(ethylene glycol) hydrogels. *Journal of biomedical materials research* **59**, 63-72 (2002).

19. Brekke, J.H. A rationale for delivery of osteoinductive proteins. *Tissue engineering* **2**, 97-114 (1996).

20. Saha, K. *et al.* Substrate modulus directs neural stem cell behavior. *Biophysical journal* **95**, 4426-38 (2008).

21. Hern, D.L. & Hubbell, J.A. Incorporation of adhesion peptides into nonadhesive hydrogels useful for tissue resurfacing. *Journal of Biomedical Materials Research* **39**, 266-276 (1998).

22. Browning, M.B., Wilems, T., Hahn, M. & Cosgriff-Hernandez, E. Compositional control of poly(ethylene glycol) hydrogel modulus independent of mesh size. *Journal of biomedical materials research. Part A* **98**, 268-73 (2011).

23. Bulick, A.S. *et al.* Impact of endothelial cells and mechanical conditioning on smooth muscle cell extracellular matrix production and differentiation. *Tissue engineering. Part A* **15**, 815-25 (2009).

24. Ford, M.C. *et al.* A macroporous hydrogel for the coculture of neural progenitor and endothelial cells to form functional vascular networks in vivo. *Proceedings of the National Academy of Sciences of the United States of America* **103**, 2512-7 (2006).

25. Watkins, A.W. & Anseth, K.S. Investigation of Molecular Transport and Distributions in Poly(ethylene glycol) Hydrogels with Confocal Laser Scanning Microscopy. *Macromolecules* **38**, 1326-1334 (2005).

26. Hummon, A.B., Lim, S.R., Difilippantonio, M.J. & Ried, T. Isolation and solubilization of proteins after TRIzol extraction of RNA and DNA from patient material following prolonged storage. *BioTechniques* **42**, 467-70, 472 (2007).

CONTACT INFORMATION

Name:	Bagrat Grigoryan
Professional Address:	c/o Dr. Mariah Hahn Department of Chemical Engineering 227 Jack E. Brown Engineering Building 3122 TAMU College Station, TX 77843-3122
Email Address:	bgrigoryan@gmail.com
Education:	B.S., Biomedical Engineering, Texas A&M University, May 2013